COMMUNICATIONS CHEMISTRY

ARTICLE

DOI: 10.1038/s42004-018-0013-3 OPEN

Formation of inclusion type silicon phases induced by inert gases

Yuanfei Bi[1], Enshi Xu[1], Timothy A. Strobel[2] & Tianshu Li[1]

Silicon clathrate, an important allotrope of silicon, has attractive opto-electronic properties for energy applications. However, it remains an experimental challenge to synthesize electrically undoped, intrinsic clathrate. Here we show, through high-throughput computer modeling, that unconventional silicon phases spontaneously nucleate from liquid silicon in the presence of noble gases under high pressure and high temperature. In particular, our results show that a medium-sized noble gas, for example, argon, can trigger the nucleation and growth of inert-gas silicon clathrate, whereas a small noble gas such as helium is able to induce the formation of an unconventional, inclusion-type compound Si_2He. The formation of both silicon phases can be attributed to the same thermodynamic and kinetic rationale that explains the crystallization of clathrate hydrate, an isostructural analog. Our findings, along with the gained molecular insights, thus strongly suggest a viable experimental synthesis route for these silicon phases using noble gases at high pressure.

[1] Department of Civil and Environmental Engineering, George Washington University, Washington, DC 20052, USA. [2] Geophysical Laboratory, Carnegie Institution of Washington, Washington, DC 20015, USA. Correspondence and requests for materials should be addressed to T.L. (email: tsli@gwu.edu)

Group IV semiconductors, namely, Si and Ge, have the well-known diamond cubic (DC) structure as their thermodynamically stable phase at ambient conditions. Although the DC structure pertains to most current technological applications, group IV semiconductors in fact also feature a very complex free energy landscape with many local minima[1]. As a result, a large number of metastable allotropes emerge when pressure and temperature are extended beyond ambient conditions. These allotropes, if synthesized under extreme conditions, may also be kinetically stabilized under ambient conditions, thus allowing potential for the exploitation of their novel properties.

Among the large number of allotropes of group IV semiconductors, open-framework structures have gained special attentions for their promising opto-electronic properties. These low-density allotropes have a rather expanded crystal structure, usually containing open channels, or polyhedral cages. Although atoms are still tetrahedrally coordinated through sp^3 bonds, the open-framework structures yield different topologies from the DC structure. Particularly, while only six-membered rings are present in the DC structure, open-frameworks can contain a variety of ring structures, for example, five-membered rings. Consequently, bonds in these low-density allotropes are distorted with respect to perfect tetrahedral geometry, and thus are expected to yield novel opto-electronic properties for solar applications[2,3]. For example, type II Si clathrate (Si_{136}) was demonstrated to have an optical band gap of 1.9 eV[4], that is, about 0.7 eV above that of DC Si. Electronic structure calculations[5,6] also suggested the band gap of Si clathrate is either direct or quasi-direct (namely, formally indirect, but the direct and indirect gaps are nearly degenerate). A recently synthesized new allotrope of silicon, Si_{24}, was identified to possess an orthorhombic lattice and to contain eight-membered rings[7]. Both experimental measurements and theoretical calculations suggested Si_{24} has a quasi-direct band gap of 1.3 eV.

Despite the novel properties of open-framework structures and the remarkable theoretical predictions for new allotropes, the synthesis of these metastable structures represents a major challenge. This is because although metastable allotropes are local minima on free energy landscape, they are usually separated by large kinetic barriers which are difficult to overcome through conventional synthesis. The use of novel precursor materials may help alleviate the problem by reducing the barrier[8]. For example, doped Si clathrates were synthesized with alkali or alkaline earth metals as guests[9], and nearly intrinsic type II Si clathrate can be obtained through thermal decomposition of Zintl monosilicide followed by a thermal degassing process to remove guests[4]. Similarly, Si_{24} was obtained by employing the precursor phase Na_4Si_{24} and sodium was subsequently removed also by a thermal degassing process[7]. However, since alkali metals are strong electronic donors, even trace amounts of atoms may significantly modify the electronic properties of intrinsic clathrate frameworks. To circumvent the problem, it is desirable to synthesize novel intrinsic group IV semiconductor allotropes involving only electrically inert elements.

Group IV clathrates are ideal systems for exploring the possibility of incorporating inert guests. A natural way of obtaining intrinsic clathrate would be the direct synthesis of empty clathrate without inclusion of guest. This certainly represents a major experimental challenge because empty clathrate was predicted to be thermodynamically stable only under negative pressure[10–12]. Another possibility is to use electrically inert guests that fit geometrically within cavities and weakly interact with the host atoms, for example, noble gas elements. Indeed, empty type II clathrate hydrate "Ice XVI", a structural analog of group IV clathrate, has been obtained by pumping neon guests out of neon hydrate[13]. To this end, theoretical studies have suggested that inert-gas-encapsulated group IV clathrate can maintain charge neutrality and thus preserves appealing opto-electronic properties of the framework[6,14,15]. Quantum chemistry calculations beyond density functional theory also indicated that the formation of these clathrates is energetically favorable[16]. However, despite the high promise and predicted high stability, experimental synthesis of these inert gas inorganic clathrate has not been reported[17].

To understand if inert gas group IV clathrates could be experimentally synthesized, it is useful to recall structurally equivalent, but chemically different crystals: clathrate hydrates. Similar to group IV clathrates, clathrate hydrates are also host–guest compounds, with the host and guest being water and gas molecules, respectively. Although the frameworks of clathrate hydrates are built by hydrogen bonds which are much weaker than the covalent bonds of group IV clathrates, both types of clathrates share the same framework structures and many physical properties. In fact, the similarity between the two clathrates can be rationalized at a fundamental level: Si, Ge, and water in fact all belong to tetrahedral materials, for their common structural motif where atoms/molecules are tetrahedrally coordinated. This common structural motif, which is also largely preserved in many non-crystalline phases of tetrahedral materials, yields unusual thermodynamic and structural properties that are shared by the group of materials. Therefore the knowledge gained from one system can be readily transferred to another.

For clathrate hydrates, the guests are usually small molecules such as hydrocarbons. A common example is methane hydrate, where methane molecules serve as the guests and fill the polyhedral water cages. Methane hydrate typically forms when methane meets water at their interface under moderate or high pressure and low temperature. Although methane is hydrophobic, and thus has a very low solubility in water, it can effectively structure its first hydration shell and yields a hydration number of 19–20 (refs. [18,19]). This coincides with the hydration number 20 for methane within the dodecahedral water cage 5^{12}, which is composed of 12 five-membered rings of water. Since the 5^{12} cage is one of the major building blocks of clathrate frameworks, the formation of methane hydrate can be promoted if there exist enough building blocks in liquid. This may be facilitated through increasing pressure or lowering temperature which allows water to dissolve more methane molecules. Therefore the structural similarity between liquid and solid in their local structures of water around a guest provides the key structural basis for inducing the formation of clathrate hydrate.

Given the intrinsic connection between clathrate hydrates and group IV clathrates, the known formation mechanism of methane hydrate may be borrowed to understand whether group IV clathrates can be formed in a similar manner. In this work, we take the first step to explore such possibility through a high-throughput computer search within a four-dimensional parameter space. Interestingly, our results show inert gases not only can induce the formation of Si clathrate, but can also yield an unconventional, inclusion-type compound Si_2He that can be viewed as a guest-filled diamond hexagonal (DH) Si structure. Both silicon phases are promising candidates for energy applications, and can find their structural analogs in methane hydrate under ambient and high pressure conditions. Importantly, the fact that both crystals are found to form spontaneously in direct molecular dynamics simulations presents strong theoretical evidence for their existence and indicates viability for the experimental synthesis of both phases.

Results

Formation of Silicon clathrate. We first begin our study by addressing the question of whether inert guests could induce the

formation of silicon clathrate when mixed with liquid silicon under pressure. Although, in principle, the question can be answered by simply examining the outcome of a direct simulation under various conditions, this heuristic approach is neither effective nor conclusive in practice. As a rare event, crystallization is usually unlikely to occur spontaneously in direct simulation unless strongly driven to become extremely fast, that is, with a crystallization rate $>10^{31}$ m^{-3} s^{-1}. This typically occurs when the nucleation barrier becomes sufficiently small, for example, under high supercooling conditions, so that the spontaneous crossing becomes frequent within the typical temporal and spatial scale of direct simulation. Alternatively, one may use an advanced sampling method, such as the forward flux sampling (FFS) method[20], to explore crystallization under more realistic conditions[21,22], but the computational cost may also be exceedingly demanding for the scope of this study.

To accelerate the exploration, we recall the isostructural relationship between group IV clathrates and gas hydrates. From a structural point of view, a good hydrate former should meet at least two criteria. First, it should be able to induce a structural ordering of host atoms/molecules resembling those of polyhedral cages in clathrate. A good indicator of this kind is the coordination number (CN) of host atoms/molecules around a guest in solution, and a good clathrate former should yield a CN close to the number of host atoms/molecules within a cage. Indeed, aqueous methane was found to have a hydration number (19–20)[18,19], very close to the number of water molecules within the dodecahedral cage of hydrate. Second, a clathrate former should also have a non-negligible solubility (χ_G) in the solution, as a clathrate nucleus cannot form without the agglomeration of a certain number of cages. This is essentially why pressure is needed in hydrate formation, to dissolve a sufficient number of guests into water. On the basis of these understandings, it is thus expected that an inorganic clathrate former should possess similar characteristics. Therefore a preliminary screening of potential clathrate formers can be carried out by examining the CN and χ_G of a guest.

The calculated CN for He at 1460 K and 1 GPa is found to be near 12.7, and it only varies slightly with temperature and pressure. Therefore, from the aforementioned viewpoint, He does not appear to be a good clathrate former. This is not unexpected because He is a small atom, which is indeed known to occupy interstitial sites of DC silicon[23,24]. In fact, as will be indicated in the next section, He is found to induce the formation of an unconventional Si–He compound with a framework of DH. As He is too small to induce Si clathrate formation, it is of interest to understand whether larger inert gas atoms can be effective clathrate formers. To answer this question, we performed a computational search of clathrate formers by systematically varying both r_0 and ε_0 in the Morse potential for describing the guest–host interaction (see Methods section). Since ε_0 and r_0 are the respective energy and length scales of such interaction, tuning both parameters mimics the properties of a wide range of noble gases with different sizes and binding energies with Si. Thus, the two characteristic scales, along with temperature T and pressure p, constitute a four-dimensional parameter space for the computational search.

The search identifies the following trends regarding χ_G and CN, as shown in Figs. 1 and 2. First, the CN of the guest is found to increase monotonically with both r_0 and ε_0, but relatively independent of T and p. Second, the solubility of the guest χ_G is found to increase with both pressure and ε_0, but to decrease with temperature and guest size r_0. The dependence of both CN and χ_G with all four variables is akin to that of small hydrophobic molecules in water[25], and indeed shares the same origin. On the one hand, the guest acts as cavity in liquid silicon, by excluding

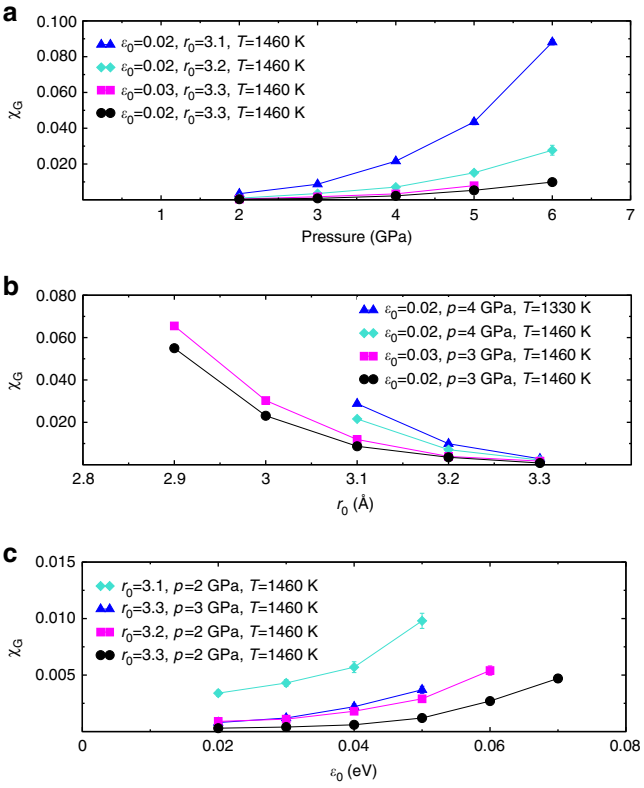

Fig. 1 Guest solubility in liquid Si. Variation of the calculated mean solubility χ_G (molar fraction) of guests in liquid Si with **a** pressure, **b** the length scale of guest–host interaction r_0, and **c** the energy scale of guest–host interaction ε_0. Error bars represent the statistical uncertainty of the calculated mean solubility, which is obtained by the block average method. The details of such estimate are explained in Supplementary Note 1 and Supplementary Fig. 1

silicon from the volume it occupies. Because guests are small enough, silicon atoms can still maintain a tetrahedral network by going around the guests without inducing dangling bonds. As a result, the first coordination shell of Si increases as such a cavity (guest) enlarges. The sovlation free energy of the guest is mainly entropic, and it increases with the size of the guest. On the other hand, the guest–host van der Waals interaction, although much weaker, can attract more Si atoms around the guest as the interaction strength increases, thus leading to an increase of both CN and χ_G with ε_0.

Figure 1 also shows that the effects from different variables (T, p, r_0, and ε_0) can generally compensate each other. For instance, the loss of solubility due to increased temperature T or guest size r_0 may be counterbalanced by increased pressure p or binding strength ε_0. Similarly, the change in CN can be offset by tuning r_0 and ε_0. However, since the CN only weakly depends on T and p, varying thermodynamic conditions may only affect the solubility for a well-defined guest (where r_0 and ε_0 are fixed).

Remarkably, a number of spontaneous clathrate nucleation and growth events are observed during the computational search. A typical trajectory of this kind is shown in Fig. 3. The crystallization event is detected by a gradual decrease of potential energy, which is a typical signature of a disorder–order transition. Subsequent analysis of the structure using the half-cage order parameter[21,22], which was developed to distinguish hydrate-like water, indeed shows that clathrate forms spontaneously. As shown in Fig. 3a, the trajectory involves an induction period

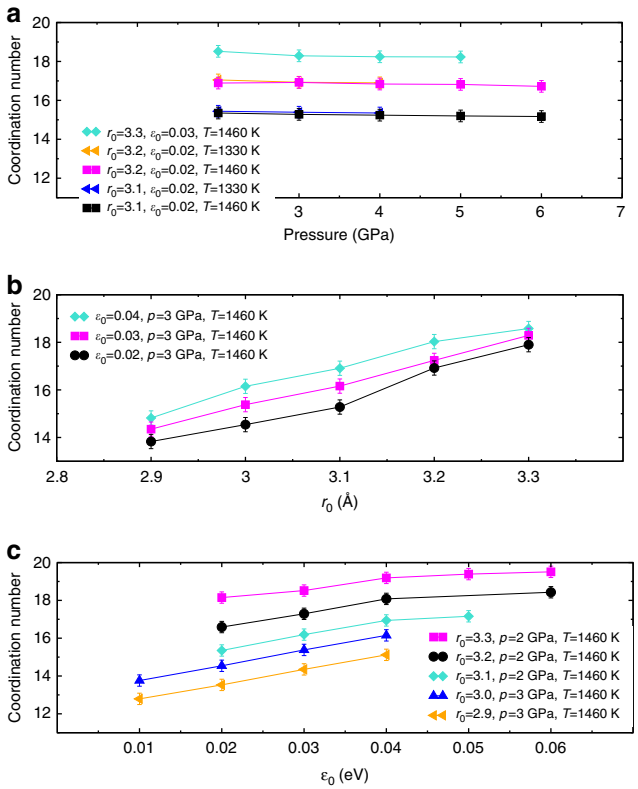

Fig. 2 Coordination number of Si around guest in liquid Si. Variation of the calculated mean coordination number of Si around guests with **a** pressure, **b** the length scale of guest-host interaction r_0, and **c** the energy scale of guest-host interaction ε_0. Error bars are defined as the standard error of the calculated mean coordination

(~2.5 ns), followed by a steady increase in the number of clathrate-like Si atoms. As shown in Fig. 3b–e, fluctuation randomly creates clathrate-like fragments within liquid Si, but nucleation and growth of clathrate only occurs at the gas/liquid interfaces. This is not surprising because the formation and aggregation of clathrate cages must be facilitated by guests, which are more abundant near the gas reservoir. Consequently, clathrate forms along two parallel interfaces, due to periodic boundary conditions, before it grows inwards, namely, along x. The anistropic growth of clathrate thus yields two layers of solid clathrate that act as barriers to diffusion for gas into the liquid. As a result, the growth of clathrate ceases as gas atoms become depleted in the liquid, leaving a diluted solution within the interior of the liquid.

Figure 4 shows nucleation maps of spontaneous formation of clathrate with respect to the variation of T, p, r_0, and ε_0. The nucleation map, along with the variation of CN and χ_G (Figs. 1 and 2), clearly reveals a few important trends and implications for clathrate formation. First, guest size plays an important role in the ability to form clathrate. While a small guest does not appear to be good clathrate former due to its low CN, a large guest may not be effective either because of its very low solubility in liquid Si. Instead, a medium-sized guest (i.e., with a guest–host distance r_0 between 3.1 and 3.4 Å) offers a good balance between both key characteristics required for a clathrate former. On the basis of the van der Waals radii of noble gases, Ar is thus projected to be a promising Si clathrate former. To further test this prediction, we employ ab initio quantum chemistry methods to compute the dissociation curves for different silicon/noble gas dimers (see Supplementary Note 3 and Supplementary Fig. 3). Our result shows that both the energy and length scales of Si–Ar interaction ($\varepsilon_0 = 0.051$ eV, $r_0 = 3.2$ Å) are indeed located well within the spontaneous nucleation map (Fig. 4), thus strongly suggesting that Ar is a good candidate for the formation of silicon clathrate. Second, for a given clathrate former, a combination of high pressure and low temperature appears to be an optimal thermodynamic condition for clathrate nucleation. This can be clearly seen from Fig. 4 where the region of spontaneous nucleation significantly expands with increasing pressure and decreasing temperature. The enhancement is primarily attributed to the increasing amount of dissolved guests in solution, which is required for clathrate formation. The suggested clathrate formation conditions are readily attainable in experiment, as pressures in the range of several GPa can be conveniently controlled using a diamond anvil cell (DAC). Finally, it is worth noting that, although a spontaneous nucleation in direct MD simulations is certainly a strong indication of clathrate formation, a non-nucleating trajectory does not necessarily imply clathrate formation is unattainable in experiments. In fact, nucleation occurring spontaneously in direct simulation implies an unrealistically high rate (>10^{31} m^{-3} s^{-1}), which is many orders of magnitude greater than a typical experimental rate (e.g., a nucleation event occurring within 1 cm^3 and 1 s yields a rate of 10^6 m^{-3} s^{-1}). Consequently, the map of clathrate nucleation (Fig. 4) in terms of an experimentally accessible scale is expected to be much larger, covering a wider range of parameters. Therefore, the results and analysis suggest that it is extremely likely to obtain Si clathrate when mixing liquid Si with medium-sized noble gases like Ar under pressure.

Formation of Si–He compound. During the search for clathrate formers, a spontaneous crystallization of Si mixed with He is identified at 1460 K and 7 GPa, as signified by the observed decrease of system potential energy, as shown in Fig. 5a. A quick view of the structure (Fig. 5f, g)) reveals that the crystallized Si framework does not resemble clathrate, but appears similar to DH silicon. Structural analysis based on the local order parameter q_6[26] indeed shows that the silicon framework corresponds to DH silicon, albeit exhibiting lattice distortions. At first glance, this is rather surprising given that the thermodynamic condition at which the spontaneous crystallization occurs falls well within the phase region of liquid Si for the SW potential[12]. In fact, the nucleation of DC silicon at the same temperature, but a much lower pressure (zero) was found to be already slow enough that it requires advanced sampling methods like FFS[27] to obtain the crystallization trajectory in simulation. Since the melting line of DC silicon has a negative slope, the nucleation rate is expected to drop exponentially with pressure, thus making it impossible to observe spontaneous crystallization of DH/DC at the examined conditions.

To understand the unexpected formation process, we examine the crystallization trajectory. As shown in Fig. 5b–e, the formation of the crystalline phase is initiated at the gas/liquid interface and propagates into the interior of liquid silicon. This appears similar to the crystallization of inert-gas clathrate, and thus implies the formation process can be a result of the guests. Interestingly, Fig. 5f, g shows the crystallization not only yields a DH-like silicon framework, but also orders guests into periodic arrays, suggesting a distinct chemical compound.

A closer structural analysis indeed shows that the new phase can be described as an inclusion-type compound with an anisotropically distorted framework of DH-like lattice encapsulating He atoms in the hexagonal channel of Si. In particular, each building block of DH Si framework, that is, diamond hexagonal core (DHC) (see Fig. 6), encloses one He atom at the interstitial site of DHC. Since a DHC is composed of 12 Si atoms, each of

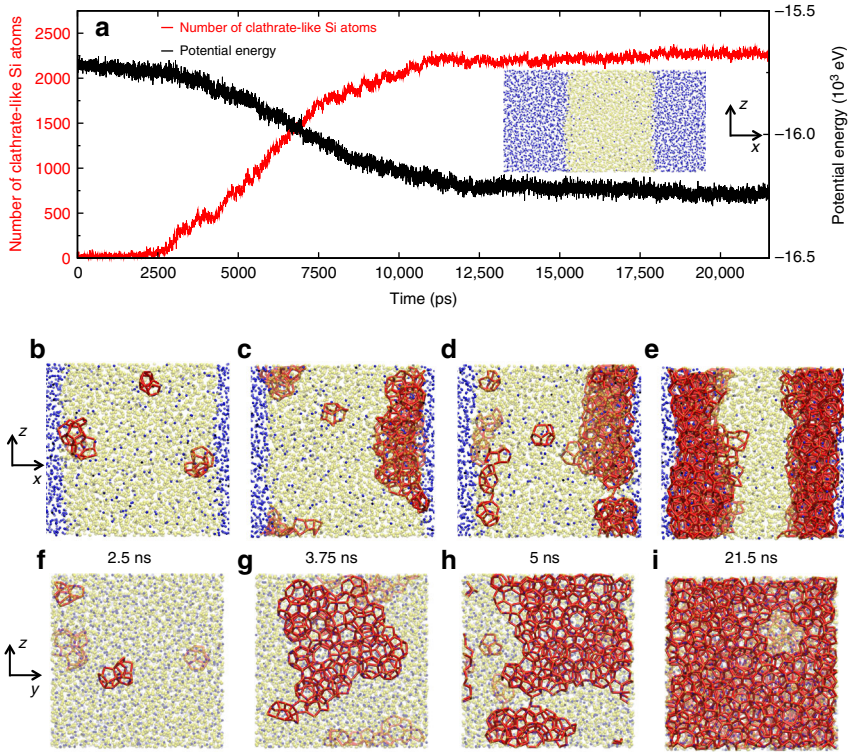

Fig. 3 Spontaneous formation of Si clathrate at 1460 K and 5 GPa. The guest has a length scale $r_0 = 3.1$ Å and energy scale $\varepsilon_0 = 0.03$ eV. **a** Time evolution of total potential energy (black) and number of clathrate-like Si atoms (red). Inset shows the side view (*xz* projection) of the simulation cell. **b**–**e** are the snapshots of the nucleation trajectory within the *xz* plane (liquid plus interfaces) at 2.5, 3.75, 5, and 21.5 ns, respectively. To facilitate another view of the same trajectory, **f**–**i** show the simulation cells at the same time sequence as in **b**–**e**, respectively, but within the *xy* plane. Silicon and guest atoms are colored by yellow and blue, respectively, and clathrate-like Si are highlighted by solid red bonds

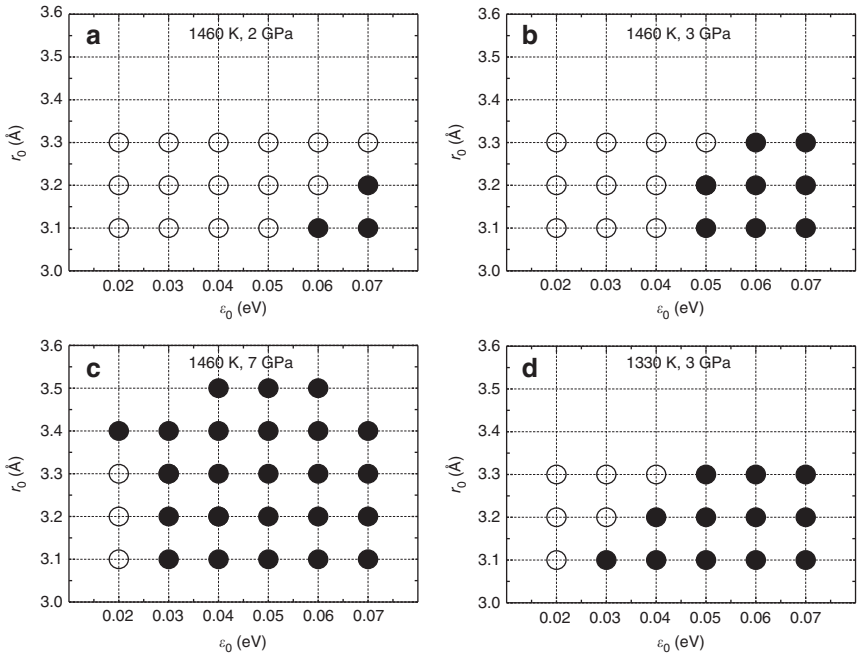

Fig. 4 Map of spontaneous clathrate formation under various conditions. Different combinations of ε_0 and r_0 (represented by circles) are tested in direct MD simulations, where clathrate is found to form spontaneously with certain guests (represented by solid circles), and no formation (represented by empty circles) is observed within a trajectory of 20 ns

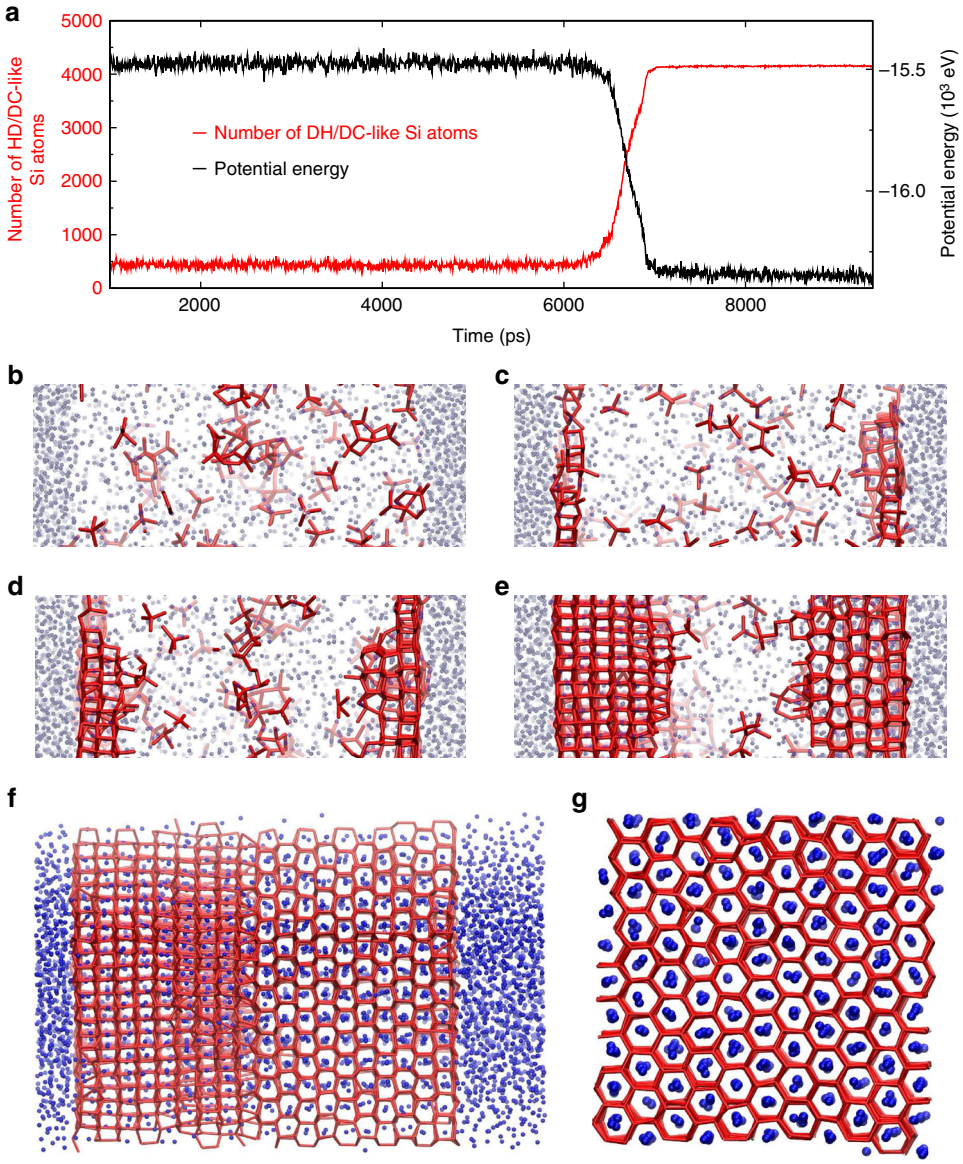

Fig. 5 Spontaneous formation of Si_2He inclusion compound at 1460 K and 7 GPa. **a** Time evolution of system potential energy and number of DH/DC-like Si atoms. **b**–**e** are the snapshots of the crystallization trajectory at 6, 6.3, 6.5, and 6.7 ns, respectively. **f** and **g** provide two views of the fully crystallized structure. Si and He are represented by red and blue, respectively

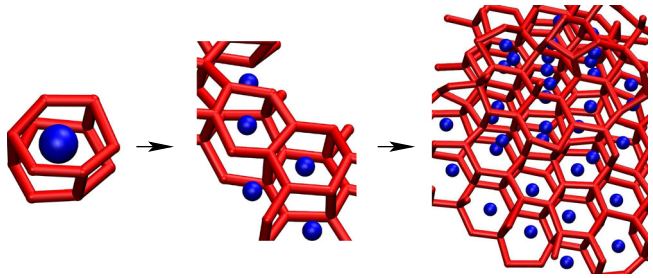

Fig. 6 Nucleation pathway of Si_2He. The nucleation of Si_2He is initiated at gas/liquid interface by forming an Si diamond hexagonal core enclosing one He atom inside. The DHC can be viewed composed of two six-membered rings as basal planes, and three six-membered rings as prismatic planes. The growth of Si_2He can proceed by attaching another DHC either on prismatic planes or on basal planes, similar to the growth of hexagonal ice I_h[44]

which is shared by six DHCs, the inclusion compound exhibits a well-defined chemical stoichiometry of Si_2He. It is noted that Si_2He also bears some resemblance to the "filled ices"[28–31] in that small guests such as hydrogen molecules or helium atoms were found to occupy the open channels of host ice lattices, which also yields a well-defined guest–host stoichiometry. Si_2He is further found to be particularly related to methane hydrate III (MH-III)[30] as both compounds share the same guest–host ratio of 1:2, and appear hexagonal-like when viewed along *c* axis (Fig. 5g). However when viewed perpendicular to the *c* axis, MH-III exhibits a different topology from hexagonal ice I_h (or DH) with four- and eight-member rings, the latter of which form a large open channel where methane molecules reside[30], whereas Si_2He appears topologically identical to DH (Fig. 5f). It is also noted that our ab initio calculation based on the GW approximation further predicts this new inclusion-type compound Si_2He to be a direct band-gap semiconductor with a gap size of ~1.1 eV, thus showing a very promising electronic property for energy

applications. The detailed analysis on its opto-electronic properties will be reported in a separate contribution.

It is then of interest to understand why and how Si_2He spontaneously nucleates from the liquid/gas mixture at a T/p condition where DH/DC silicon is thermodynamically unstable. Energetically speaking, this question appears particularly intriguing because the host–guest interaction (~7.7 meV) is very weak compared to the host–host interaction (2.17 eV, that is, the well depth of the two-body term of the SW potential). To rationalize our results, it is useful to again recall the water–methane system. Although hydrogen bonds in water are about eight times weaker than Si–Si bonds, they are still two orders of magnitude stronger than water–methane interactions. In this system, the existence of methane in water not only induces the formation of a different crystal from ice, but also shifts the water/ice phase boundary substantially[32]. From a kinetic point of view, the formation of methane hydrate can be attributed to the solvation of water around methane, which leads to a water structure in close resemblance to hydrate. As discussed above, this also explains the formation of inert-gas Si clathrate. Similarly, a small guest such as He is found to yield an Si CN of 12.7, very close to the number of Si atoms in DHC (12) enclosing He in Si_2He. Therefore, the presence of a sufficient number of He atoms in liquid Si provides a strong structural basis for the formation of Si_2He. Indeed, the molecular nucleation pathway (Figs. 5 and 6) shows an Si DHC enclosing one He atom emerging at the liquid/gas interface, with its basal plane parallel to the interface. This DHC thus provides six anchoring sites for attaching DHCs in plane, which leads to growth parallel to the interface, and one anchoring site for growing DHC out-of-plane towards the liquid.

The spontaneous formation of Si_2He compound can be also understood from a thermodynamic point of view. To this end, we estimate the equilibrium melting line of the Si_2He phase by employing the two-phase approach[33] (see Supplementary Note 4 and Supplementary Fig. 4). As shown in Fig. 7, the calculated melting line of Si_2He is found to shift significantly with respect to that of DC/DH. In particular, the calculated melting temperature of Si_2He at 7 GPa is around 1925 ± 25 K, that is, about 550 K above that of DC/DH. Notably, the melting line of Si_2He also exhibits a positive slope, indicating a volume increase upon melting. This is in contrast to DC/DH which is less dense than its liquid, that is, a typical behavior of tetrahedral materials. The change of melting curve and the sign of melting-line slope can be attributed to the incorporation of guest atoms within the structure, leading to a denser packing in the crystalline phases, which can also find strong analogy to the water–gas systems[29,32]. Therefore, at 7 GPa, the temperature (1460 K) where crystallization occurs spontaneously corresponds to a supercooling of 23–25%. This is in fact a typical condition to observe homogeneous nucleation in a direct MD simulation[34,35].

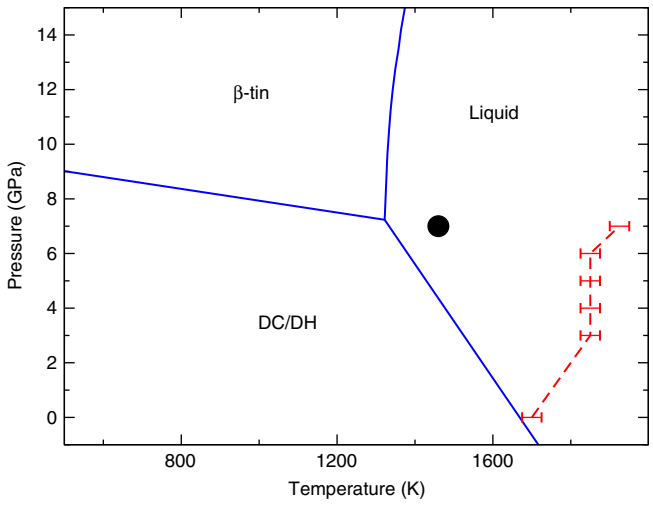

Fig. 7 Melting line of Si_2He. The thermodynamic condition (marked as a black dot) where spontaneous formation of Si_2He occurs in MD falls within the phase region of liquid SW Si. Blue lines are the phase boundaries extracted from the calculated $T-p$ phase diagram of SW silicon[12]. The calculated equilibrium phase boundary of Si_2He is represented by a red dashed line, with an uncertainty of temperature of ±25 K

Discussion

Inspired by the need for synthesizing novel, silicon-based energy materials with intrinsic semiconducting properties, we carried out theoretical and computational studies to explore the kinetics and thermodynamics for the formation of novel phases composed of Si and noble gases. The potential advantage of employing noble gas to form novel silicon phases over the traditional method by thermal decomposition of Zintl precursor is obvious as noble gas can keep the desired electronic properties of Si clathrate largely intact. Therefore the key question is to assess whether a weak guest–host interaction is possible to divert the formation pathway of the strongly bonded host lattice to form a stable/metastable phase, for example, clathrate.

Encouragingly, our computational search indeed shows this is very likely under high pressure and high temperature. The computational search within a four-dimensional parameter space indicates that the two key metrics for clathrate formation, namely, CN of host around guest and solubility of guest in host liquid, can be optimized by varying pressure, temperature, guest size, and guest–host interaction strength. Remarkably, inert-gas silicon clathrate is indeed found to crystallize spontaneously at the gas/liquid interface within nanoseconds in direct molecular dynamics simulations, strongly indicating the likelihood for clathrate formation under high pressure and temperature. In particular, a medium-sized noble gas such as Ar is projected to have the right interaction strength to trigger Si clathrate formation, as further confirmed by our high-fidelity quantum chemistry calculation.

Another intriguing finding of this study is the spontaneous formation of an unexpected inclusion-type of compound Si_2He, which is not only the first stoichiometric compound composed of these elements, but also is predicted to be a direct band-gap semiconductor. Although small guests appear insufficient to structure the liquid Si shell to be clathrate-like, it yields a local structural motif reminiscent to DH lattice, thus kinetically favoring the formation of the inclusion compound. This spontaneous formation can also be rationalized thermodynamically from the calculated melting curve of Si_2He, which is significantly distinct from that of DC/DH silicon.

The study has been motivated and guided by our knowledge gained in hydrocarbon–water systems. Apart from the apparent structural similarities between clathrate hydrates and group IV clathrates, the two systems are in fact connected at a more fundamental level: The tendency of preserving local tetrahedral coordination ensures a strong analogy between the two chemically distinct systems. Small hydro- and silicon-phobic guests thus essentially act as a small cavity in the tetrahedral network, which can go around the cavity while still maintaining tetrahedral coordination without inducing dangling bonds. As a result, with different guest sizes and interactions, host atoms/molecules around guests may exhibit different topologies that locally match various crystalline phases. This serves as one of the structural bases for the formation of novel guest–host phases. Not only clathrate phases exist in both systems, but the predicted

compound Si_2He can also find its structural analog with the high-pressure filled ices. From this viewpoint, and given that a variety of hydrate structures have been discovered under both ambient and high pressure[36], we expect there should also exist rich phase behaviors of group IV/inert gas systems, particularly under high pressure.

It is also worth noting that, despite the strong analogy between them, water and silicon are indeed distinguished in their tetrahedrality[37] and bonding nature of the framework, which may subsequently yield important implications for experimental synthesis. For example, the strong covalent Si–Si bond (about one order of magnitude stronger than water hydrogen bond) implies the corresponding energy scale must be much higher in the silicon system than in water for the similar types of structures and phase transitions. The difference in bonding may also lead to a stronger guest–host repulsion in the silicon-guest system under pressure. Consequently, high pressure (GPa) and high temperature (>1000 K) are inevitably required for the formation of inert-gas Si phases. Therefore the experimental synthesis of novel Si allotropes with inert gas may be carried out through the melting Si in DAC filled with noble gases.

Finally, we note that as the main scope of the work is to explore the kinetic formation pathways, a large body of the study is carried out based on classical force fields to access the necessary length and time scales of such processes. Although some of the key guest–host interactions used in the work can be verified by our quantum chemistry calculations at the MP2 level, the fidelity of the prediction can be further enhanced by employing a higher level theory such as coupled cluster. More importantly, the thermodynamic stability of the predicted new phases, in particular, the pressure range within which these phases are stable, should be examined by an accurate quantum chemistry approach. Further studies are thus needed to understand the enthalpy difference between the predicted structures and those competing phases under high pressure.

Methods

Force fields. Our molecular simulations are carried out using the Stillinger–Weber (SW) model of silicon[38]. The SW model is one of the most widely used force fields for group IV semiconductors in describing their solid and liquid phases. Given the intrinsic similarity among tetrahedral materials, the SW model has also been successfully extended to the water/ice system through representing water molecules as monoatomic particles with a tetrahedral strength intermediate between those of silicon and carbon[39]. Very recently, the phase diagram of silicon has been calculated over a wide temperature and pressure range[12]. Silicon–gas interaction, which is mediated through van der Waals (vdW) force, is modeled by a simple Morse potential $\Phi(r) = \varepsilon_0\left[\left(1 - e^{-k(r-r_0)^2}\right) - 1\right]$, where ε_0 is the well depth (energy scale), r_0 is the equilibrium binding distance (length scale), and k represents the width of the well. For the silicon–helium system, the parameters are obtained through fitting against the potential developed for silicon–helium[40], by tuning k while fixing $\varepsilon_0 = 7.7$ meV and $r_0 = 2.912$ Å (these numbers correspond to the energy and length scale of the potential). The fitting yields $k = 2.06994$ Å^{-2}, which reproduces the potential almost exactly. The helium–helium interaction is represented by a Lennard-Jones (LJ) potential with $\varepsilon = 0.94$ meV and $\sigma = 2.64$ Å[41]. As there is a lack of accurate experimental data for the interactions between Si and other noble gases, we carry out our study over a range of parameters by systematically varying ε_0 and r_0, and further verify them for noble gases by quantum chemistry calculations. When varying the guest–host interaction ε_0 and r_0, the corresponding guest–guest interaction is then obtained by applying the Lorentz–Berthelot rules on the basis of the helium–helium and silicon–helium interactions. It is noted that the variation of guest–guest interaction is indeed found to have little effect on the formation of clathrate, because guests are well separated in both solution and solid so that their interactions are much smaller than guest–host interactions.

Molecular dynamics simulations. MD simulation typically involves 4192 silicon atoms and 4000 guest atoms. A larger system (containing ~13,000 Si and ~9000 guests) is also used to cross check size effects. The initial configurations are obtained by melting a silicon crystal and randomly converting a certain number of Si atoms into guests. The systems are then equilibrated at the target conditions for at least 20 ns, leading to a mixture of liquid solution and gas phase separated by two flat liquid/gas interfaces, as a result of a periodic boundary condition. At each condition, the solubility of guest in liquid Si and the partial radial distribution function $g_{GH}(r)$ are calculated based on a simulation trajectory of 30–40 ns (see Supplementary Note 2 and Supplementary Fig. 2). The CN of Si around guest is obtained by integrating $4\pi r^2 g_{GH}(r)$ up to the first local minimum. To account for the concentration gradient of guest near interfaces, a liquid slab with a thickness of 8 Å is excluded from the calculation of both solubility and CN. The statistical uncertainty for the calculated mean solubility is estimated based on the block average method[42]. More calculation details for the block average method can be found in Supplementary Note 1.

Identification of solid Si. To identify clathrate-like Si atoms in liquid, we employ the half-cage order parameter (H-COP)[21,22]. H-COP was developed to distinguish hydrate-like water molecules in liquid on the basis of topological analysis of the tetrahedral network, by identifying half polyhedral cages of water molecules, namely, the unique building blocks of clathrate hydrates. Given the structural equivalency between Si clathrate and clathrate hydrate, H-COP is thus adopted with a reduced cutoff distance of 2.7 Å. To identify DH/DC-like Si, a local order parameter q_6[26] is employed, such that an Si atom is deemed DH/DC-like when $q_6 > 0.5$. The local order parameter q_6 has been demonstrated effective in recognizing local cubic and hexagonal ordering in both ice[43] and Si[27].

Data availability. The data that support the findings of this study are available from the corresponding author upon reasonable request.

Received: 11 January 2018 Accepted: 23 January 2018
Published online: 22 March 2018

References

1. Haberl, B., Strobel, T. A. & Bradby, J. E. Pathways to exotic metastable silicon allotropes. *Appl. Phys. Rev.* **3**, 040808 (2016).
2. Botti, S., Flores-Livas, J. A., Amsler, M., Goedecker, S. & Marques, M. A. L. Low-energy silicon allotropes with strong absorption in the visible for photovoltaic applications. *Phys. Rev. B* **86**, 121204 (2012).
3. Amsler, M., Botti, S., Marques, M. A. L., Lenosky, T. J. & Goedecker, S. Low-density silicon allotropes for photovoltaic applications. *Phys. Rev. B* **92**, 014101 (2015).
4. Gryko, J. et al. Low-density framework form of crystalline silicon with a wide optical band gap. *Phys. Rev. B* **62**, R7707 (2000).
5. Adams, G. B., O'Keeffe, M., Demkov, A. A., Sankey, O. F. & Huang, Y.-M. Wide-band-gap Si in open fourfold-coordinated clathrate structures. *Phys. Rev. B* **49**, 8048–8053 (1994).
6. Blase, X. Quasiparticle band structure and screening in silicon and carbon clathrates. *Phys. Rev. B Condens. Matter* **67**, 035211 (2003).
7. Kim, D. Y., Stefanoski, S., Kurakevych, O. O. & Strobel, T. A. Synthesis of an open-framework allotrope of silicon. *Nat. Mater.* **14**, 169–173 (2014).
8. Guloy, A. M. et al. A guest-free germanium clathrate. *Nature* **443**, 320–323 (2006).
9. Kasper, J. S., Hagenmuller, P., Pouchard, M. & Cros, C. Clathrate structure of silicon Na_8Si_{46} and Na_xSi_{136} (x<11). *Science* **150**, 1713–1714 (1965).
10. Wilson, M. & McMillan, P. F. Crystal-liquid phase relations in silicon at negative pressure. *Phys. Rev. Lett.* **90**, 135703 (2003).
11. Jacobson, L. C., Hujo, W. & Molinero, V. Thermodynamic stability and growth of guest-free clathrate hydrates: a low-density crystal phase of water. *J. Phys. Chem. B* **113**, 10298–10307 (2009).
12. Romano, F., Russo, J. & Tanaka, H. Novel stable crystalline phase for the Stillinger-Weber potential. *Phys. Rev. B* **90**, 014204 (2014).
13. Falenty, A., Hansen, T. C. & Kuhs, W. F. Formation and properties of ice XVI obtained by emptying a type sII clathrate hydrate. *Nature* **516**, 231–233 (2014).
14. Connétable, D. Structural and electronic properties of p-doped silicon clathrates. *Phys. Rev. B* **75**, 125202 (2007).
15. Khabibullin, A. R., Huan, T. D., Nolas, G. S. & Woods, L. M. Cage disorder and gas encapsulation as routes to tailor properties of inorganic clathrates. *Acta Mater.* **131**, 475–481 (2017).
16. Karttunen, A. J. & Fässler, T. F. Semiconducting clathrates meet gas hydrates: $Xe_{24}[Sn_{136}]$. *Chem. Eur. J.* **20**, 6693–6698 (2014).
17. Krishna, L. & Koh, C. A. Inorganic and methane clathrates: versatility of guest–host compounds for energy harvesting. *MRS Energy Sustain.* **2**, E8 (2015).
18. Dec, S. F., Bowler, K. E., Stadterman, L. L., Koh, C. A. & Sloan, E. D. Direct measure of the hydration number of aqueous methane. *J. Am. Chem. Soc.* **128**, 414–415 (2006).
19. DeJong, P. H. K., Wilson, J. E., Neilson, G. W. & Buckingham, A. D. Hydrophobic hydration of methane. *Mol. Phys.* **91**, 99–104 (2010).

20. Allen, R. J., Frenkel, D. & Wolde, P. R. T. Simulating rare events in equilibrium or nonequilibrium stochastic systems. *J. Chem. Phys.* **124**, 024102 (2006).
21. Bi, Y. & Li, T. Probing methane hydrate nucleation through the forward flux sampling method. *J. Phys. Chem. B* **118**, 13324–13332 (2014).
22. Bi, Y., Porras, A. & Li, T. Free energy landscape and molecular pathways of gas hydrate nucleation. *J. Chem. Phys.* **145**, 211909 (2016).
23. Luther, L. C. & Moore, W. J. Diffusion of helium in silicon, germanium, and diamond. *J. Chem. Phys.* **41**, 1018–1026 (1964).
24. Alatalo, M., Puska, M. J. & Nieminen, R. M. First-principles study of He in Si. *Phys. Rev. B* **46**, 12806–12808 (1992).
25. Chandler, D. Interfaces and the driving force of hydrophobic assembly. *Nature* **437**, 640–647 (2005).
26. Li, T., Donadio, D. & Galli, G. Nucleation of tetrahedral solids: a molecular dynamics study of supercooled liquid silicon. *J. Chem. Phys.* **131**, 224519 (2009).
27. Li, T., Donadio, D., Ghiringhelli, L. M. & Galli, G. Surface-induced crystallization in supercooled tetrahedral liquids. *Nat. Mater.* **8**, 726–730 (2009).
28. Londono, D., Kuhs, W. F. & Finney, J. L. Enclathration of helium in ice II: The first helium hydrate. *Nature* **332**, 141–142 (1988).
29. Vos, W., Finger, L., Hemley, R. & Mao, H. Novel H_2-H_2O clathrates at high pressures. *Phys. Rev. Lett.* **71**, 3150–3153 (1993).
30. Loveday, J. S., Nelmes, R. J., Guthrie, M., Klug, D. D. & Tse, J. S. Transition from cage clathrate to filled ice: the structure of methane hydrate III. *Phys. Rev. Lett.* **87**, 215501 (2001).
31. Strobel, T. A., Somayazulu, M., Sinogeikin, S. V., Dera, P. & Hemley, R. J. Hydrogen-stuffed, quartz-like water ice. *J. Am. Chem. Soc.* **138**, 13786–13789 (2016).
32. Sloan, E. D. J. Fundamental principles and applications of natural gas hydrates. *Nature* **426**, 353–359 (2003).
33. Morris, J. R., Wang, C. Z., Ho, K. M. & Chan, C. T. Melting line of aluminum from simulations of coexisting phases. *Phys. Rev. B* **49**, 3109–3115 (1994).
34. Jacobson, L. C., Hujo, W. & Molinero, V. Amorphous precursors in the nucleation of clathrate hydrates. *J. Am. Chem. Soc.* **132**, 11806–11811 (2010).
35. Moore, E. B. & Molinero, V. Structural transformation in supercooled water controls the crystallization rate of ice. *Nature* **479**, 506–508 (2011).
36. Loveday, J. S. & Nelmes, R. J. High-pressure gas hydrates. *Phys. Chem. Chem. Phys.* **10**, 937–950 (2008).
37. Molinero, V., Sastry, S. & Angell, C. A. Tuning of tetrahedrality in a silicon potential yields a series of monatomic (metal-like) glass formers of very high fragility. *Phys. Rev. Lett.* **97**, 075701 (2006).
38. Stillinger, F. H. & Weber, T. A. Computer simulation of local order in condensed phases of silicon. *Phys. Rev. B Condens. Matter* **31**, 5262–5271 (1985).
39. Molinero, V. & Moore, E. B. Water modeled as an intermediate element between carbon and silicon. *J. Phys. Chem. B* **113**, 4008–4016 (2009).
40. Pizzagalli, L., David, M. L. & Bertolus, M. Molecular dynamics simulation of the initial stages of He bubbles formation in silicon. *Model. Simul. Mater. Sci. Eng.* **21**, 065002 (2013).
41. Talu, O. & Myers, A. L. Reference potentials for adsorption of helium, argon, methane, and krypton in high-silica zeolites. *Colloids Surf. A Physicochem. Eng. Asp.* **187-188**, 83–93 (2001).
42. Allen, M. & Tildesley, D. *Computer Simulation of Liquids* (Clarendon Press, Oxford, 1987).
43. Li, T., Donadio, D., Russo, G. & Galli, G. Homogeneous ice nucleation from supercooled water. *Phys. Chem. Chem. Phys.* **13**, 19807–19813 (2011).
44. Haji-Akbari, A. & Debenedetti, P. G. Direct calculation of ice homogeneous nucleation rate for a molecular model of water. *Proc. Natl. Acad. Sci. USA* **112**, 10582–10588 (2015).

Acknowledgements

We gratefully thank Prof. Hanning Chen for his assistance on quantum chemistry calculations. This work is supported by Energy Frontier Research in Extreme Environments (EFree) Center, an Energy Frontier Research Center funded by the U.S. Department of Energy, Office of Science under award number DE-SC0001057.

Author contributions

T.L. and T.A.S. conceived the research project. T.L. designed the research project. Y.B., E.X., and T.L. performed and analyzed the simulations. All authors contributed to the interpretation of the results. Y.B. and T.L. wrote the paper with contributions from E.X. and T.A.S.

Additional information

Supplementary information accompanies this paper at https://doi.org/10.1038/s42004-018-0013-3.

Competing interests: The authors declare no competing interests.

Reprints and permission information is available online at http://npg.nature.com/reprintsandpermissions/

Publisher's note: Springer Nature remains neutral with regard to jurisdictional claims in published maps and institutional affiliations.